# 11 Nonlinear control structure with direct decoupling for wind power plants with DFIM

## 11.1 Existing problems at linear controlled wind power plants

An important criterion for the design of the control concept is to maintain the decoupling of active and reactive power in both steady state and dynamic mode. This requirement is fulfilled to a very high degree by using a rotor current controller (cf. chapter 10 or [Quang 1997]) to impress control variables (rotor current components) which immediately inject torque and power factor (cf. figure 10.4). This structure, in which the current controller is always based on DFIM models linearized within a sampling period, was successfully implemented in wind power plants. The linearization is made by the assumption that the sampling time $T$ of the discretization is chosen small enough so that the rotor frequency $\omega_r$ can be regarded as constant within $T$. Because of this assumption the frequency $\omega_r$ is now a parameter in the system matrix of the discrete process model, and the bilinear continuous model becomes a linear time-variant system for which the well known design methods of linear systems can be used.

Nowadays most grid suppliers request ride-through of the wind turbine during grid faults (short-circuits, ref. to [Dittrich 2003]). That means the wind power plant must be able to feed reactive power into the grid to support the retaining voltage level, and the rotor frequency $\omega_r$ becomes very dynamic. In these cases, in which the linearization condition can not be fulfilled any more, a nonlinear design for the rotor current control loop would be able to deliver better results than the linear controller. Within the last few years a number of efforts had been made on this issue from both theoretical and practical [Chi 2005], [Quang 2005]. They succeeded – as in the case of the IM and PMSM – in a new control structure with direct decoupling between the $dq$ axes using the method of the exact linearization.

## 11.2 Nonlinear control structure for wind power plants with DFIM

In the section 3.6.3 the nonlinear process model of the DFIM was already developed as the starting point for the controller design.

$$\begin{cases} \dot{\mathbf{x}} = \mathbf{f}(\mathbf{x}) + \mathbf{h}_1(\mathbf{x})u_1 + \mathbf{h}_2(\mathbf{x})u_2 + \mathbf{h}_3(\mathbf{x})u_3 \\ \mathbf{y} = \mathbf{g}(\mathbf{x}) \end{cases} \tag{11.1}$$

with:

$$\mathbf{f}(\mathbf{x}) = \begin{bmatrix} -ax_1 \\ -ax_2 \\ 0 \end{bmatrix}; \mathbf{h}_1(\mathbf{x}) = \begin{bmatrix} 1 \\ 0 \\ 0 \end{bmatrix}; \mathbf{h}_2(\mathbf{x}) = \begin{bmatrix} 0 \\ 1 \\ 0 \end{bmatrix}; \mathbf{h}_3(\mathbf{x}) = \begin{bmatrix} x_2 \\ -x_1 \\ 1 \end{bmatrix} \tag{11.2}$$

$$g_1(\mathbf{x}) = x_1;\ g_2(\mathbf{x}) = x_2;\ g_3(\mathbf{x}) = x_3$$

- Parameters:

$$a = \left(\frac{1}{\sigma T_r} + \frac{1-\sigma}{\sigma T_s}\right); b = \frac{1-\sigma}{\sigma}; c = \frac{1}{\sigma L_r}; d = \frac{1-\sigma}{\sigma L_m}; e = \frac{1-\sigma}{\sigma T_s}$$

- State variables:

$$\mathbf{x}^T = \begin{bmatrix} x_1 & x_2 & x_3 \end{bmatrix}; x_1 = i_{rd}; x_2 = i_{rq}; x_3 = \theta_r$$

- Input variables:

$$\mathbf{u}^T = \begin{bmatrix} u_1 & u_2 & u_3 \end{bmatrix}; u_1 = e\psi_{sd}' - b\omega\psi_{sq}' + cu_{rd} - du_{sd}$$

$$u_2 = b\omega\psi_{sd}' + e\psi_{sq}' + cu_{rq} + du_{sq}; u_3 = \omega_r$$

- Output variables:

$$\mathbf{y}^T = \begin{bmatrix} y_1 & y_2 & y_3 \end{bmatrix}; y_1 = i_{rd}; y_2 = i_{rq}; y_3 = \theta_r$$

### 11.2.1 Nonlinear controller design based on "exact linearization"

The design is made similarly as in the case of the IM.

- Step 1: Calculation of the vector **r**.

a) Case $j = 1$:

$$L_{h_1} g_1(\mathbf{x}) = \frac{\partial g_1(\mathbf{x})}{\partial \mathbf{x}} \mathbf{h}_1(\mathbf{x}) = \begin{bmatrix} 1 & 0 & 0 \end{bmatrix} \begin{bmatrix} 1 \\ 0 \\ 0 \end{bmatrix} = 1 \neq 0 \tag{11.3a}$$

$$L_{h_2} g_1(\mathbf{x}) = \frac{\partial g_1(\mathbf{x})}{\partial \mathbf{x}} \mathbf{h}_2(\mathbf{x}) = \begin{bmatrix} 1 & 0 & 0 \end{bmatrix} \begin{bmatrix} 0 \\ 1 \\ 0 \end{bmatrix} = 0 \tag{11.3)b}$$

$$L_{h_3} g_1(\mathbf{x}) = \frac{\partial g_1(\mathbf{x})}{\partial \mathbf{x}} \mathbf{h}_3(\mathbf{x}) = \begin{bmatrix} 1 & 0 & 0 \end{bmatrix} \begin{bmatrix} x_2 \\ -x_1 \\ 1 \end{bmatrix} = x_2 \neq 0 \tag{11.3)c}$$

From (11.3) it results $r_1 = 1$.

b) Case $j = 2$:

$$L_{h_1} g_2(\mathbf{x}) = \frac{\partial g_2(\mathbf{x})}{\partial \mathbf{x}} \mathbf{h}_1(\mathbf{x}) = \begin{bmatrix} 0 & 1 & 0 \end{bmatrix} \begin{bmatrix} 1 \\ 0 \\ 0 \end{bmatrix} = 0 \tag{11.4)a}$$

$$L_{h_2} g_2(\mathbf{x}) = \frac{\partial g_2(\mathbf{x})}{\partial \mathbf{x}} \mathbf{h}_2(\mathbf{x}) = \begin{bmatrix} 0 & 1 & 0 \end{bmatrix} \begin{bmatrix} 0 \\ 1 \\ 0 \end{bmatrix} = 1 \neq 0 \tag{11.4)b}$$

$$L_{h_3} g_2(\mathbf{x}) = \frac{\partial g_2(\mathbf{x})}{\partial \mathbf{x}} \mathbf{h}_3(\mathbf{x}) = \begin{bmatrix} 0 & 1 & 0 \end{bmatrix} \begin{bmatrix} x_2 \\ -x_1 \\ 1 \end{bmatrix} = -x_1 \neq 0 \tag{11.4)c}$$

Therewith it follows $r_2 = 1$.

c) Case $j = 3$:

$$L_{h_1} g_3(\mathbf{x}) = \frac{\partial g_3(\mathbf{x})}{\partial \mathbf{x}} \mathbf{h}_1(\mathbf{x}) = \begin{bmatrix} 0 & 0 & 1 \end{bmatrix} \begin{bmatrix} 1 \\ 0 \\ 0 \end{bmatrix} = 0 \tag{11.5)a}$$

$$L_{h_2} g_3(\mathbf{x}) = \frac{\partial g_3(\mathbf{x})}{\partial \mathbf{x}} \mathbf{h}_2(\mathbf{x}) = \begin{bmatrix} 0 & 0 & 1 \end{bmatrix} \begin{bmatrix} 0 \\ 1 \\ 0 \end{bmatrix} = 0 \tag{11.5)b}$$

$$L_{h_3} g_3(\mathbf{x}) = \frac{\partial g_3(\mathbf{x})}{\partial \mathbf{x}} \mathbf{h}_3(\mathbf{x}) = \begin{bmatrix} 0 & 0 & 1 \end{bmatrix} \begin{bmatrix} x_2 \\ -x_1 \\ 1 \end{bmatrix} = 1 \neq 0 \tag{11.5)c}$$

With the equation (11.5) $r_3 = 1$ is obtained now.

- Step 2: Calculation of the matrix .

$$\mathbf{L}(\mathbf{x}) = \begin{bmatrix} L_{h_1} g_1(\mathbf{x}) & L_{h_2} g_1(\mathbf{x}) & L_{h_3} g_1(\mathbf{x}) \\ L_{h_1} g_2(\mathbf{x}) & L_{h_2} g_2(\mathbf{x}) & L_{h_3} g_2(\mathbf{x}) \\ L_{h_1} g_3(\mathbf{x}) & L_{h_2} g_3(\mathbf{x}) & L_{h_3} g_3(\mathbf{x}) \end{bmatrix} = \begin{bmatrix} 1 & 0 & x_2 \\ 0 & 1 & -x_1 \\ 0 & 0 & 1 \end{bmatrix} \tag{11.6}$$

Therewith it is: $\det\left[\mathbf{L}(\mathbf{x})\right]=1\neq 0 \quad \forall\mathbf{x}$

- Step 3: Realization of the coordinate transformation.

a) The state space $\mathbf{x}$ is transformed into a new state space $\mathbf{z}$ using the equation (9.4). After replacing $r_1 = r_2 = r_3 = 1$ into (9.4), the same result like (9.11) for the case IM and (9.25) for the case PMSM will be obtained:

$$\mathbf{z}=\begin{bmatrix} z_1 \\ z_2 \\ z_3 \end{bmatrix}=\begin{bmatrix} m_1^1(\mathbf{x}) \\ m_1^2(\mathbf{x}) \\ m_1^3(\mathbf{x}) \end{bmatrix}=\begin{bmatrix} g_1(\mathbf{x}) \\ g_2(\mathbf{x}) \\ g_3(\mathbf{x}) \end{bmatrix}=\begin{bmatrix} x_1 \\ x_2 \\ x_3 \end{bmatrix} \tag{11.7}$$

The equations (9.11), (9.25) and (11.7) show that the new state variables are identical to the old ones, and therefore the physically fundamental properties of the system "electrical machines IM, PMSM and DFIM" remain unchanged after the transformation of state coordinates.

b) The new state model is the same as (9.12) and (9.26):

$$\begin{cases} \dfrac{dz_1}{dt}=\dfrac{\partial g_1(\mathbf{x})}{\partial \mathbf{x}}\dfrac{d\mathbf{x}}{dt}=L_f g_1(\mathbf{x})+L_{h_1} g_1(\mathbf{x})u_1+L_{h_2} g_1(\mathbf{x})u_2+L_{h_3} g_1(\mathbf{x})u_3 \\ \dfrac{dz_2}{dt}=\dfrac{\partial g_2(\mathbf{x})}{\partial \mathbf{x}}\dfrac{d\mathbf{x}}{dt}=L_f g_2(\mathbf{x})+L_{h_1} g_2(\mathbf{x})u_1+L_{h_2} g_2(\mathbf{x})u_2+L_{h_3} g_2(\mathbf{x})u_3 \\ \dfrac{dz_3}{dt}=\dfrac{\partial g_3(\mathbf{x})}{\partial \mathbf{x}}\dfrac{d\mathbf{x}}{dt}=L_f g_3(\mathbf{x})+L_{h_1} g_3(\mathbf{x})u_1+L_{h_2} g_3(\mathbf{x})u_2+L_{h_3} g_3(\mathbf{x})u_3 \end{cases} \tag{11.8}$$

with:

$$\begin{cases} L_f g_1(\mathbf{x})=\dfrac{\partial g_1(\mathbf{x})}{\partial \mathbf{x}} f(\mathbf{x})=\begin{bmatrix}1 & 0 & 0\end{bmatrix}\begin{bmatrix}-ax_1 \\ -ax_2 \\ 0\end{bmatrix}=-ax_1 \\ L_f g_2(\mathbf{x})=\dfrac{\partial g_2(\mathbf{x})}{\partial \mathbf{x}} f(\mathbf{x})=\begin{bmatrix}0 & 1 & 0\end{bmatrix}\begin{bmatrix}-ax_1 \\ -ax_2 \\ 0\end{bmatrix}=-ax_2 \\ L_f g_3(\mathbf{x})=\dfrac{\partial g_3(\mathbf{x})}{\partial \mathbf{x}} f(\mathbf{x})=\begin{bmatrix}0 & 0 & 1\end{bmatrix}\begin{bmatrix}-ax_1 \\ -ax_2 \\ 0\end{bmatrix}=0 \end{cases}$$

These terms have to be inserted into the equation (11.8), and the result of the transformation will be obtained to:

$$\begin{aligned}
\frac{dz_1}{dt} &= -ax_1 + u_1 + x_2 u_3 = w_1 \\
\frac{dz_2}{dt} &= -ax_2 + u_2 - x_1 u_3 = w_2 \\
\frac{dz_3}{dt} &= u_3 = w_3
\end{aligned} \tag{11.9}$$

From the equation (11.9) the new input vector **w** is given as follows:

$$\mathbf{w} = \begin{bmatrix} w_1 \\ w_2 \\ w_3 \end{bmatrix} = \underbrace{\begin{bmatrix} -ax_1 \\ -ax_2 \\ 0 \end{bmatrix}}_{\mathbf{p}(\mathbf{x})} + \underbrace{\begin{bmatrix} 1 & 0 & x_2 \\ 0 & 1 & -x_1 \\ 0 & 0 & 1 \end{bmatrix}}_{\mathbf{L}(\mathbf{x})} \underbrace{\begin{bmatrix} u_1 \\ u_2 \\ u_3 \end{bmatrix}}_{\mathbf{u}} \tag{11.10}$$

- Step 4: The control law results from (11.10) as follows.

$$\mathbf{u} = \underbrace{-\mathbf{L}^{-1}(\mathbf{x})\mathbf{p}(\mathbf{x})}_{\mathbf{a}(\mathbf{x})} + \mathbf{L}^{-1}(\mathbf{x})\mathbf{w} = \mathbf{a}(\mathbf{x}) + \mathbf{L}^{-1}(\mathbf{x})\mathbf{w}$$

$$= \begin{bmatrix} u_1 \\ u_2 \\ u_3 \end{bmatrix} = \underbrace{\begin{bmatrix} \left(\dfrac{1}{\sigma T_r} + \dfrac{1-\sigma}{\sigma T_s}\right) x_1 \\ \left(\dfrac{1}{\sigma T_r} + \dfrac{1-\sigma}{\sigma T_s}\right) x_2 \\ 0 \end{bmatrix}}_{\mathbf{a}(\mathbf{x})} + \underbrace{\begin{bmatrix} 1 & 0 & -x_2 \\ 0 & 1 & x_1 \\ 0 & 0 & 1 \end{bmatrix}}_{\mathbf{L}^{-1}(\mathbf{x})} \underbrace{\begin{bmatrix} w_1 \\ w_2 \\ w_3 \end{bmatrix}}_{\mathbf{w}} \tag{11.11}$$

### 11.2.2 Feedback control structure with direct decoupling for DFIM

Similarly to the cases IM and PMSM and using the state feedback (11.11), the exactly linearized DFIM model is represented in the figure 11.1. It can be easily recognized that also here – like for IM – only the submodel of the rotor current is linearized exactly. In the case IM it was the submodel of the stator current. Both equations (9.11) and (11.7) express this clearly.

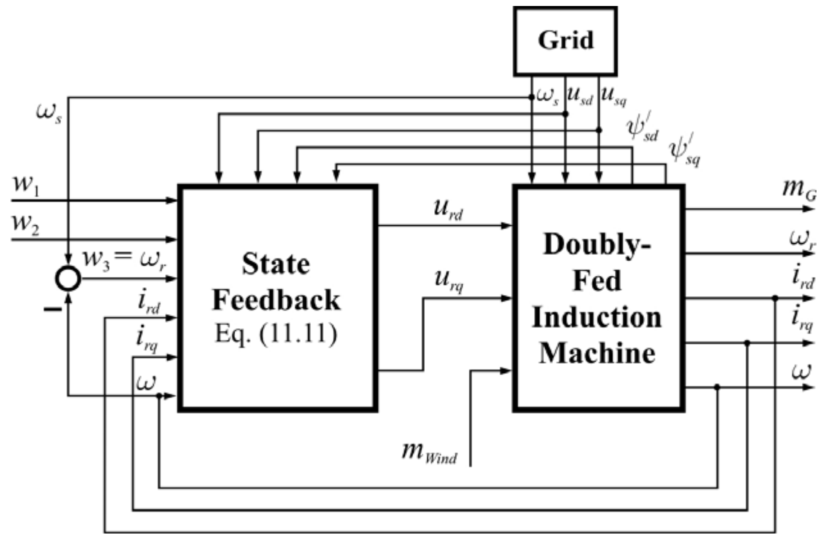


**Fig. 11.1** Substitute linear process model of the DFIM

The new linear process model of the DFIM is identical to the model expressed by the equation (9.18) and the comments to (9.18). Using the coordinate transformation (11.11) or the structure in the figure 11.1, the new generator-side control scheme can be derived as in the figure 11.2.

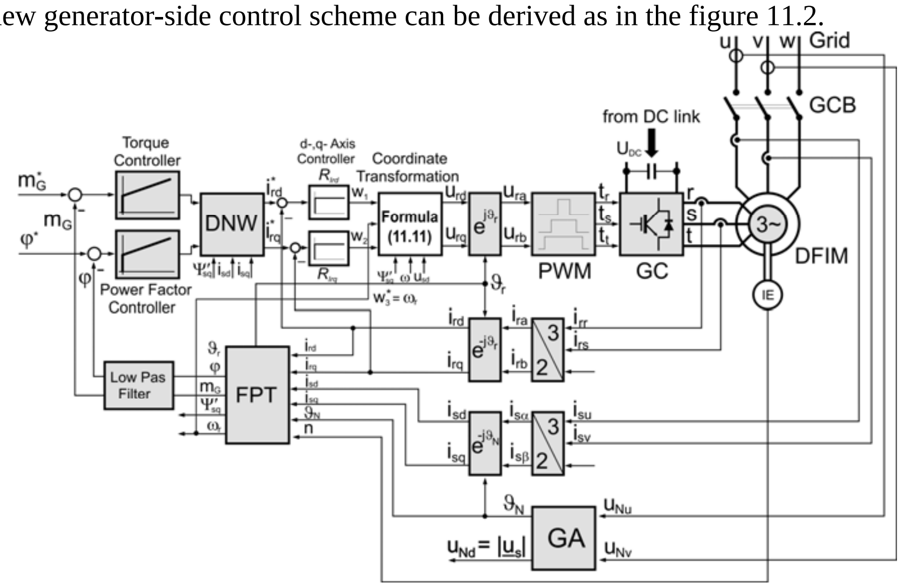


**Fig. 11.2** Generator-side control scheme using exact linearization by state coordinate transformation and two separate axis controllers to impress current components

To verify the capabilities of the newly proposed nonlinear control scheme, a series of simulations (cf. [Quang 2005]) have been performed. Results are shown below in figure 11.3 for the case of step changes in the grid voltage of different amplitudes. This special test procedure has been chosen due to the following considerations:

- Generator systems are required to stay operational during grid voltage faults (fault ride-through, FRT). The control system should be capable to maintain this operability as far as possible to avoid falling back to hardware protection circuitry to ensure FRT.
- From the control point of view, a grid voltage step change poses a strong disturbance to the system where its qualities can clearly be revealed.

In the simulations, the results for a linear control system according to figure 10.4 and the nonlinear scheme outlined above are compared for 3 different voltage steps to 70%, 50% and 25% retained grid voltage. Both control schemes had been implemented into an otherwise identical converter-generator system of a 2500 kW wind power plant. Fore sole comparison of the control systems, hardware protection and FRT features had been excluded deliberately.

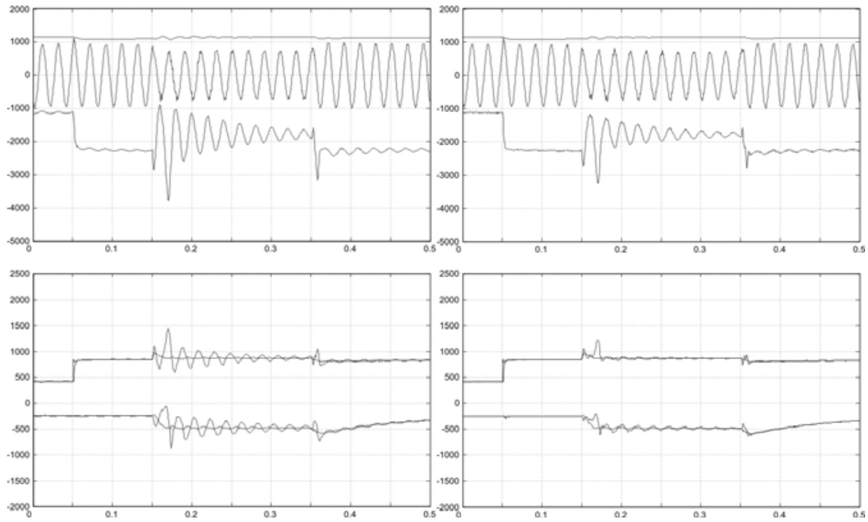

**Fig. 11.3a** Grid voltage drop to 70% retaining voltage, 2500 kW converter-generator system: (**left**) linear control scheme, (**right**) nonlinear control scheme, (**top**) Speed [rpm], grid voltage [V], torque [10 Nm], (**bottom**) rotor current d (torque) [A], rotor current q (flux) [A]

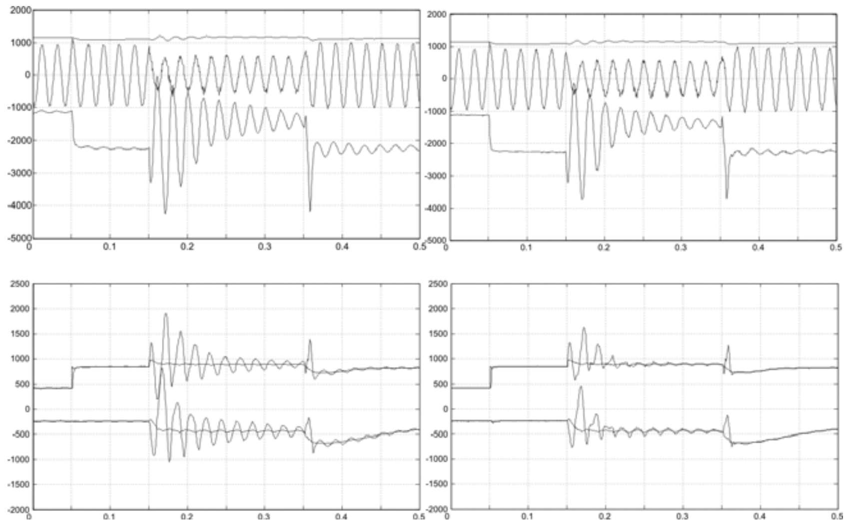

**Fig. 11.3b** Grid voltage drop to 50% retaining voltage, quantities like figure 11.3a

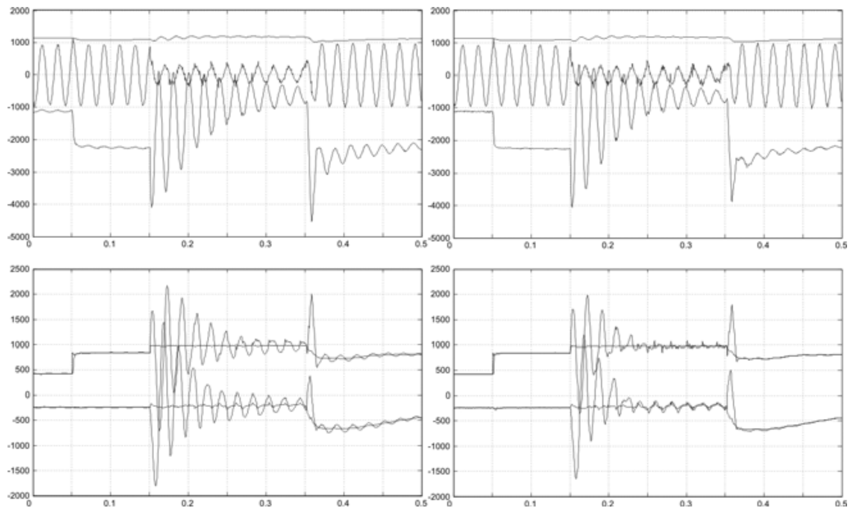

**Fig. 11.3c** Grid voltage drop to 25% retaining voltage, quantities like figure 11.3a

For the examination of the control behaviour two different time spans must be distinguished: Immediately after the voltage step, the system will lose its controllability due to limitation of the rotor voltage. The performance here depends on how effective the limited voltage is assigned to the respective d- and q-components. After the voltage limitation is overcome and the system controllability regained, the performance can be judged from how fast the rotor currents are forced to follow their set points again.

The results show that the new direct decoupling concept clearly outperforms the linear control in both aspects:

- Smaller oscillation amplitudes of stator and rotor currents occur in the first milliseconds after the fault instant while the rotor current controllers work in limitation mode. This means practically, that the system may cope with more serious fault events without triggering hardware protection functions.
- The system control functionality is regained very fast after the controllers return to linear operation, resulting in short recovery time from disturbances and continuation of defined control behaviour.

These results of simulation were also confirmed by a practical laboratory implementation [Lan 2006]. It should be mentioned also, that the differences between linear and nonlinear control with respect to torque behaviour are considerably less pronounced. This had to be expected, since the nonlinear decoupling has been developed with respect to rotor current, where the performance difference is clearly visible. To extend the nonlinear approach also to flux and torque control will be a matter of further research.

## 11.3 References to chapter 11

Bodson M, Chiasson J (1998) Differential-Geometric Methods for Control of Electric Motors. Int. J. Robust Nonlinear Control 8, pp. 923-954

Chi PL, Tuan NQ (2005) Design of a Nonlinear Control Algorithm with Direct Decoupling for Wind Power Plant Using DFIM and Validation by Simulation with MATLAB & Simulink and PLECS. Bachelor Thesis (in Vietnamese), Hanoi University of Technology.

Dawson DM, Hu J, Burg TC (2004) Nonlinear Control of Electric Machinery. Marcel Dekker, Inc., New York Basel

Dittrich JA, Stoev A (2003) Grid Fault Proof Doubly-Fed Induction Generator System. EPE Toulouse

Khorrami F, Krishnamurthy P, Melkote H (2003) Modeling and Adaptive Nonlinear Control of Electric Motors. Springer, Berlin Heidelberg New York

Krstíc M, Kanellakopoulos I, Kokotovíc P (1995) Nonlinear and Adaptive Control Design. John Wiley & Sons, Inc., New York

Lan PN (2006) Linear and Nonlinear Control Approach of Doubly-Fed Induction Generator in Wind Power Generation. Dissertation, TU Dresden

Ortega R, Loría A, Nicklasson PJ, Sira-Ramírez H (1998) Passivity-based Control of Euler-Lagrange Systems: Mechanical, Electrical and Electromechanical Applications. Springer, London Berlin Heidelberg

Phuoc ND (2005) Combining of Exact Linearization and Model Reference Techniques for Design of Adaptive GAS Controller and Application to Adaptive Control of Induction Motor. Intern. Conf. CD Proc. of 11th European Conf. on Power Electronics and Applications, 11-14 Sept., Dresden

Quang NP (2004) Nonlinear Control Structures: New Application Perspective in 3-Phase AC Drives. Proc. of the 8th Intern. Conf. on Mechatronics Technology ICMT, November 8-12, Hanoi, pp. 213 – 219

Quang NP, Dittrich JA (1999) Praxis der feldorientierten Drehstromantriebs-regelungen. 2. Aufl., Expert-Verlag

Quang NP, Dittrich A, Lan PN (2005) Doubly-Fed Induction Machine as Generator in Wind Power Plant: Nonlinear Control Algorithms with Direct Decoupling. Intern. Conf. CD Proc. of 11th European Conf. on Power Electronics and Applications, 11-14 Sept., Dresden

Quang NP, Dittrich A, Thieme A (1997) Doubly-Fed Induction Machine as Generator: Control Algorithms with Decoupling of Torque and Power Factor. Electrical Engineering / Archiv für Elektrotechnik, 10.1997, pp. 325-335

Wey T (2001) Nichtlineare Regelungssysteme: Ein differentialalgebraischer Ansatz. B.G. Teubner Stuttgart - Leipzig - Wiesbaden.